# On metrics and models for multiplex networks

Gemmetto, V.

# Chapter 1

# Undirected multiplex networks

Several systems can be represented as multiplex networks, i.e. in terms of a superposition of various graphs, each related to a different mode of connection between nodes. Hence, the definition of proper mathematical quantities aiming at capturing the added level of complexity of those systems is required. Various steps in this direction have been made. In the simplest case, dependencies between layers are measured via correlation-based metrics, a procedure that we show to be equivalent to the use of completely homogeneous benchmarks specifying only global constraints. However, this approach does not take into account the heterogeneity in the degree and strength distributions, which is instead a fundamental feature of real-world multiplexes. In this chapter, we compare the observed dependencies between layers with the expected values obtained from maximum-entropy reference models that appropriately control for the observed heterogeneity in the degree and strength distributions. This information-theoretic approach results in the introduction of novel and improved multiplexity measures that we test on different datasets, i.e. the International Trade Network and the European Airport Network. Our findings confirm that the use of homogeneous benchmarks can lead to misleading results, and highlight the important role played by the distribution of hubs across layers.

The results presented in this chapter have been published in the following reference:
V. Gemmetto, D. Garlaschelli, *Scientific Reports*, **5**, 9120 (2015).

## 1.1 Introduction

The study of networks allows scientists to suitably represent and analyze biological, economic and social systems as a set of units (nodes) connected by edges (links) symbolizing interactions [1, 2, 3, 4].

However, this approach may actually lead to an oversimplification: indeed, several systems are composed by units connected by multiple kinds of interaction. In such systems, the same set of nodes is joined by various types of links, each of those representing a different mode of connection [5]. The simplest way to analyse such systems is the aggregation of the various levels in a single network, but it turns out that such a simplification may discard fundamental information about the real topology of the network and therefore about possible dynamical processes acting on the system [6]. For instance, such an aggregation may result in a loss of information about the distribution of the hubs across layers, which is instead crucial for the control of several processes arising on an interdependent network [7]. Then, in order to solve such an issue, in the last few years the study of multi-layer networks has been pursued. In this context, new quantities aiming at mathematically analyzing multi-level networks have been provided [8, 9, 10, 11]; furthermore, models of growth [12, 13, 14] and dynamical processes occurring on multiplexes, such as epidemic spreading [15], diffusion [16], cooperation [17] and information spreading [18] have been designed.

In this chapter, we follow the path towards the definition of measures that can be applied to multi-level networks, in order to characterize significant structural properties of these systems, in particular focusing on the analysis of the dependencies between layers. We argue that, in order to properly characterize such dependencies, a comparison between the observed correlation and some notion of expected correlation is required. We therefore exploit the concept of multiplex ensemble [19, 20, 21], aiming at the definition of suitable null models for multi-layer complex networks, in order to compare the observed overlap between layers with the expected overlap one would find in a random superposition of layers with the same node-specific properties. In particular, since our purpose is precisely that of measuring such dependencies, we will consider uncorrelated multiplex ensembles, in order to define a null model for the real system so that it is possible to compare the observed correlations with reference models where the overlap between layers is actually randomized and, at the same time, important node-specific properties of the real network are preserved.

Various efforts have already been made about the study of correlations in multi-level networks [22, 23, 24], but the comparison of the observed results with the expected ones has generally been based on a - sometimes implicit - assumption: the benchmark was a completely homogeneous graph. In particular, here we show that correlation-based measures of inter-layer dependency (of the type used e.g. in ref.[22]) build on an implicit assumption of homogeneity, which in the unweighted case is equivalent to the choice of the Random Graph as null model. Similarly, for weighted networks, the chosen benchmark was equivalent to the Weighted

Random Graph, where the weight distribution is independent from the considered pair of nodes [25].

However, this assumption of uniformity in the probability distributions strongly contrasts with the observed findings in real-world complex systems. Indeed, one of the most well-known features of complex networks is their heterogeneity [26], both in the degree distribution and in the strength distribution; it is therefore crucial to take this aspect into account when proper null models for graphs are designed. Moreover, it has been recently shown that, in multiplex networks, the correlation between degrees (and strengths) of nodes across different layers is also an important structural feature that can have strong effects on the dynamics [7, 27]. Ultimately, such inter-layer degree correlations determine the distribution of hubs across layers, i.e. whether the same nodes tend to be hubs across many layers, or whether different layers are characterized by different hubs. We therefore aim at measuring multiplexity in terms of the "residual" inter-layer dependencies that persist after we filter out, for each layer separately, the effects induced by the heterogeneity of the empirical degree (for unweighted networks) or strength (for weighted graphs) distribution. We show that such a refinement can completely change the final findings and lead to a deeper understanding of the actual dependencies observed between layers of a real-world multiplex.

First, we introduce a new *"absolute" measure of multiplexity* designed to quantify the overlap between layers of a multi-level complex network. Second, we derive the expression of the expected value of such a quantity, both in the binary and in the weighted case, for randomized networks, by enforcing different constraints. Third, we combine the "absolute" multiplexity and its expected value into a *filtered, "relative" measure of multiplexity* that has the desired properties. We finally apply our measures to two different real-world multiplexes, namely the World Trade Multiplex Network and the European Airport Network, showing that the analysis of the dependencies between layers can actually make some important structural features of these systems explicit.

Indeed, while the former shows significant correlations between layers (i.e., traded commodities), in the latter almost no overlap can generally be detected, thus clearly defining two opposite classes of multiplexes based on the observed correlations. Furthermore, we will link such a behaviour with the distribution of the hubs across layers, hence providing a straightforward explanation to the observed findings.

## 1.2 Methods

### 1.2.1 Null models

It is possible to design null models for multi-level networks as maximum-entropy ensembles on which we enforce a given set of constraints [21]. In particular, we exploit the concept of uncorrelated multiplex ensemble, so that the definition of

proper null models for the considered multiplex reduces to the definition of an indipendent null model for any layer of the system. In order to do this, we take advantage of the concept of canonical network ensemble, or exponential random graph [28], i.e. the maximum-entropy family of graphs satisfying a set of constraints on average. In this context the resulting randomized graph preserves only part of the topology of the considered real-world network and is entirely random otherwise, thus it can be employed as a proper reference model. However, fitting such previously defined models to real datasets is hard, since it is usually computationally demanding as it requires the generation of many randomized networks whose properties of interest have to be measured.

In this perspective, we exploit a fast and completely analytical maximum-entropy method, based on the maximization of the likelihood function [29, 30, 31], which provides the exact probabilities of occurrence of random graphs with the same average constraints as the real network. From such probabilities it is then possible to compute the expectation values of the properties we are interested in, such as the average link probability or the average weight associated to the link established between any two nodes. While the adoption of such a method is not strictly required when dealing with global constraints like the total number of links observed in a network (the so-called Random Graph), it becomes crucial when facing the problem of enforcing local constraints such as the degree sequence or the strength sequence (Binary or Weighted Configuration Model). More information about such null models can be found in the following subsections and appendices.

### 1.2.2 Homogeneous null models

The simplest null model for a binary multiplex is an independent superposition of layers in which each layer is a Random Graph (RG) [28], which enforces as constraint the expected number of links in that layer. Such model, therefore, provides a unique expected probability $p^\alpha$ that a link between any two nodes is established in layer $\alpha$: however, such a reference model completely discards any kind of heterogeneity in the degree distributions of the layers, resulting in graphs where each node has on average the same number of connections, inconsistently with the observed real networks. Thus, the probability of connection between any two nodes in layer $\alpha$ is uniformly given by:

$$p^\alpha = \frac{L^\alpha}{N(N-1)/2} \tag{1.1}$$

where $L^\alpha$ is the total number of links actually observed in layer $\alpha$.

Similar considerations apply to weighted networks and the related Weighted Random Graph (WRG) [25], i.e. the straightforward extension of the previous Random Graph to weighted systems; in such a null model, the probability of having a link of weight $w$ between two nodes $i$ and $j$ is independent from the choice of the nodes and only depends on the total weight observed in a layer and on the number of nodes.

Analogously to the corresponding Binary Random Graph, also this kind of null model discards the simultaneous presence of nodes with high and low values of the strengths (that is, a high or low sum of the weights associated to links incident on that node).

### 1.2.3 Heterogeneous null models

To take into account the heterogeneity of the real-world networks, in the unweighted case we consider a null model where the multiplex is an independent superposition of layers, each of which is a (Binary) Configuration Model (BCM) [32], i.e. an ensemble of networks satisfying on average the empirical degree sequence observed in that specific layer. Since we make use of the canonical ensembles, it is possible to obtain from the maximum-likelihood method each probability $p_{ij}^{\alpha}$ that nodes $i$ and $j$ are connected in layer $\alpha$ (notice that such value $p_{ij}^{\alpha}$ is basically the expectation value of $a_{ij}^{\alpha}$ under the chosen Configuration Model). Similarly, as a null model for a weighted multiplex we consider an independent superposition of layers, each described by the Weighted Configuration Model (WCM) [33]: here, for each layer separately, the enforced constraint is the strength sequence as observed in the real-world multiplex. In this view, the likelihood maximization provides the expectation value of each weight $w_{ij}^{\alpha}$ for any pair of nodes $i$ and $j$ as supplied by the Weighted Configuration Model. It is worth noticing that enforcing the degree sequence (respectively, the strength sequence in the weighted case) automatically leads to the design of a null model where also the total number of links (respectively, the total weight) of the network is preserved. In the appendices attached to this chapter we will provide equations generalizing, for instance, equation (1.1), whose solution allows then to derive the analytical expression of the expected link probability $p_{ij}^{\alpha}$ and, in the weighted case, the expected link weight $w_{ij}^{\alpha}$. In order to do this, we make use of a set of $N$ auxiliary variables $x_i^{\alpha}$ for any layer $\alpha$, which are proportional to the probability of establishing a link between a given node $i$ and any other node (or, respectively for the weighted case, establishing a link characterized by a given weight), being therefore directly informative on the expected probabilities $p_{ij}^{\alpha}$ (or, respectively, the expected weights $w_{ij}^{\alpha}$).

Before introducing our measures of multiplexity, we make an important preliminary observation. Simple measures of inter-layer dependency are based on correlation metrics, which in turn rely on an assumption of uniformity, such assumption being ultimately equivalent to the choice of a uniform Random Graph as a null model; this will strengthen the choice of emplying heterogeneous benchmarks throughout the entire thesis. We illustrate this result in more detail in the appendices.

### 1.2.4 Multiplexity

When unweighted networks are considered, we define the "absolute" binary multiplexity between any two layers $\alpha$ and $\beta$ as:

$$m_b^{\alpha\beta} = \frac{2\sum_{i<j}\min\{a_{ij}^{\alpha}, a_{ij}^{\beta}\}}{L^{\alpha} + L^{\beta}} \tag{1.2}$$

where $L^{\alpha}$ is the total number of links observed in layer $\alpha$ and $a_{ij}^{\alpha} = 0, 1$ depending on the presence of the link between nodes $i$ and $j$ in layer $\alpha$. Such a quantity represents a normalized overlap between any pair of layers and can therefore be thought of as a normalized version of the global overlap introduced in [21].

The previous definition can be easily extended to weighted multiplex networks. We define the "absolute" weighted multiplexity as:

$$m_w^{\alpha\beta} = \frac{2\sum_{i<j}\min\{w_{ij}^{\alpha}, w_{ij}^{\beta}\}}{W^{\alpha} + W^{\beta}} \tag{1.3}$$

where $w_{ij}^{\alpha}$ represents the weight of the link between nodes $i$ and $j$ in layer $\alpha$ and $W^{\alpha}$ is the total weight related to the links in that layer. Both (1.2) and (1.3) range in $[0, 1]$, are maximal when layers $\alpha$ and $\beta$ are identical - that is, if there is complete similarity between those two layers - and minimal when they are totally different; in this perspective, they evaluate the tendency of nodes to share links in distinct layers.

However, the above absolute quantities are uninformative without a comparison with the value of multiplexity obtained when considering a null model. We may indeed measure high values of multiplexity between two layers due to the possibly large observed values of density, without any significant distinction between real dependence and overlap imposed by the presence of many links in each layer (thus forcing an increase in the overlap itself).

Furthermore, we cannot draw a clear conclusion about the amount of correlation between layers by just looking at the observed value, since such a measure is not universal and, for instance, no comparison between different multiplexes can be done based on the raw "absolute" multiplexity.

We therefore introduce the following "relative" or rescaled quantity along the lines of refs. [34, 35]:

$$\mu^{\alpha\beta} = \frac{m^{\alpha\beta} - \langle m^{\alpha\beta}\rangle}{1 - \langle m^{\alpha\beta}\rangle} \tag{1.4}$$

where $m^{\alpha\beta}$ is the value measured for the observed real-world multiplex and $\langle m^{\alpha\beta}\rangle$ is the value expected under a suitably chosen null model. The main null models that we will consider are respectively the Random Graph (RG) and the Binary Configuration Model (BCM) in the unweighted case, the Weighted Random Graph (WRG) and the Weighted Configuration Model (WCM) in the weighted case. We will characterize them in more detail in the appendices following this chapter.

This rescaled quantity is now directly informative about the real correlation between layers: in this context, positive values of $\mu^{\alpha\beta}$ represent positive correlations, while negative values are associated to anticorrelated pairs of layers; furthermore, pairs of uncorrelated layers show multiplexity values comparable with 0.
One of the motivations of the present work is the consideration that, in the binary case, when the Random Graph is considered as a null model, the previous quantity (1.4) can actually be reduced to the standard correlation coefficient between the entries of the adjacency matrix referred to any two layers $\alpha$ and $\beta$ of a multi-level graph, defined as:

$$Corr\{a_{ij}^{\alpha}, a_{ij}^{\beta}\} = \frac{\langle a_{ij}^{\alpha} a_{ij}^{\beta}\rangle - \langle a_{ij}^{\alpha}\rangle\langle a_{ij}^{\beta}\rangle}{\sigma_{\alpha}\sigma_{\beta}} \tag{1.5}$$

In the appendices, we show that the previous expression is nothing but a different normalization of the rescaled binary multiplexity defined in (1.4):

$$Corr\{a_{ij}^{\alpha}, a_{ij}^{\beta}\} = F\cdot\left(m^{\alpha\beta} - \langle m^{\alpha\beta}\rangle\right) \tag{1.6}$$

where $F$ is a factor depending on $L^{\alpha}$, $L^{\beta}$ and $N$.

## 1.3 Results

### 1.3.1 Binary analysis

We validate our definitions applying them to two different real-world multiplexes: the World Trade Multiplex (WTM) ($N = 207$ countries, $M = 96$ layers representing traded commodities), available as a weighted multi-level network, and the European Airport Network ($N = 669$ airports, $M = 130$ airlines), provided as an unweighted system. A more detailed description of the International Trade dataset, which is one of the main focuses of the entire thesis, can be found in the appendix following this chapter.

The implementation of the concept of multiplexity to different networks can lead to completely divergent results, according to the structural features of the considered systems. Indeed, the application of (1.2) to the WTM leads to the color-coded multiplexity matrix $\mathbf{M}_b$ shown in Figure 1.1(a). Such an array generally shows very high overlaps between layers, i.e. between different classes of commodities, pointing out that usually each country tends to import from or export to the same set of countries almost independently of the traded items; this is true in particular for most of the edible products (layers characterized by commodity codes ranging from 1 to 22, as listed in the aforementioned appendix.

In order to have a complete picture of the dependencies between layers of the considered systems, we have to compare our findings with the overlaps expected for multiplexes having only some of the properties in common with the observed ones. The simplest benchmark, as well as the most widely used, is the Random Graph (RG), which discards, as we said, any kind of heterogeneity in the degree

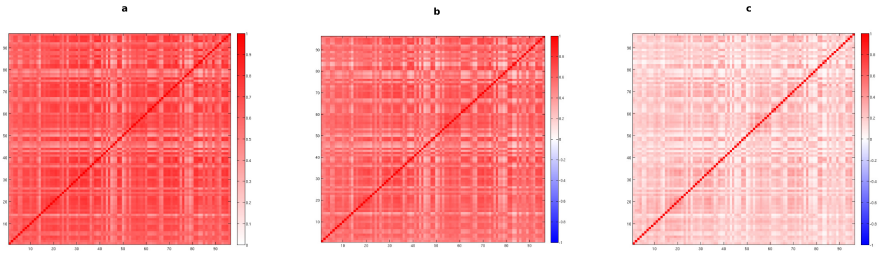


Figure 1.1: **Analysis of the binary multiplexity between layers of the World Trade Multiplex in 2011.** Color-coded matrices with entries given by $m_b^{\alpha\beta}$ (a), $\mu_{RG}^{\alpha\beta}$ (b) and $\mu_{BCM}^{\alpha\beta}$ (c) for any pair of layers (commodities).

distributions of the layers. When we compute $\mu_{RG}^{\alpha\beta}$ for the World Trade Network, we obtain the multiplexity matrix shown in Figure 1.1(b). The plot clearly shows that most of the correlations are still present: this layer-homogeneous null model, together with the presence of comparable densities across the various layers, does not significantly affect the expected overlaps. So far, we have discarded heterogeneity in our null models. However, this can considerably affect the significance of our findings. Therefore, we introduce heterogeneity in the degree distribution within the reference model by means of the previously defined (Binary) Configuration Model (BCM). This way, it is actually possible to detect only the non-trivial dependencies, therefore discarding all the overlaps simply due to the possibly high density of the layers, that would otherwise increase the observed interrelations even if no real correlation is actually present.

This is exactly what happens when the World Trade Network is analyzed. Indeed, as shown in Figure 1.1(c), we find out that a significant amount of the binary overlap observed in this network is actually due to the information included in the degree sequence of the various layers, rather than to a real dependence between layers. This method is therefore able to detect the really meaningful similarity between layers, discarding the trivial overlap caused by the presence, for instance, of nodes having a high number of connections in most of the layers. This non-significant overlap is thus filtered out by our procedure. Such observations clearly show that the Random Graph is not the most proper reference model in order to obtain an appropriate representation of crucial properties of such multilevel systems.

We now note that linear correlations have been used in the literature to produce dendrograms [22, 36]. As we mentioned, the use of linear correlations corresponds to the choice of the Random Graph as null model. Here, we can instead make use of $\mu_{BCM}^{\alpha\beta}$ to implement an improved hierarchical clustering procedure,

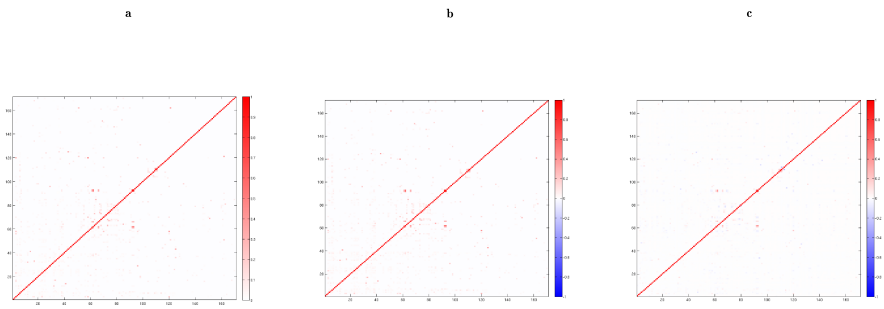


Figure 1.2: **Analysis of the binary multiplexity between layers of the European Airport Network.** Color-coded matrices with entries given by $m_b^{\alpha\beta}$ (a), $\mu_{RG}^{\alpha\beta}$ (b) and $\mu_{BCM}^{\alpha\beta}$ (c) for any pair of layers (airlines).

as reported in the appendix.

A completely different behaviour can be observed for the European Airport System. Indeed, low values of multiplexity observed for such a network (Figure 1.2(a)) illustrate nearly no overlap between most of the layers: this highlights the well-known tendency of airline companies to avoid superpositions between routes with other airlines. In Figure 1.2(b) we show the residual correlations obtained after the application of the Random Graph: almost no difference can be perceived with respect to Figure 1.2(a), since the expected overlap in this case is very small, due to the very low densities of the various layers. We should point out that the Random Graph is not a proper reference model for this real-world network, since the assumption of uniformity in the degree of the different nodes (i.e., airports) is actually far from the observed structure of such a system, as we will highlight later. Nevertheless, in Figure 1.2(c) we show that, at first glance, the adoption of the Configuration Model does not look strictly required when the European Airport Network is considered, except for a more suitable mathematical approach, since the overall matrix looks apparently similar to the previous Figure 1.2(b). However, the presence of a larger number of negative values of multiplexity and the simultaneous disappearance of most of the significantly high values highlight once more the anti-correlated character of such a system, and this crucial structural property of the airport multiplex network was not fully revealed by the application of the Random Graph.

In this case, a dendrogram designed form matrices reported in Figure 1.2 would not be meaningful, since most of the layers meet at a single root level, due to the very low correlation observed between them.

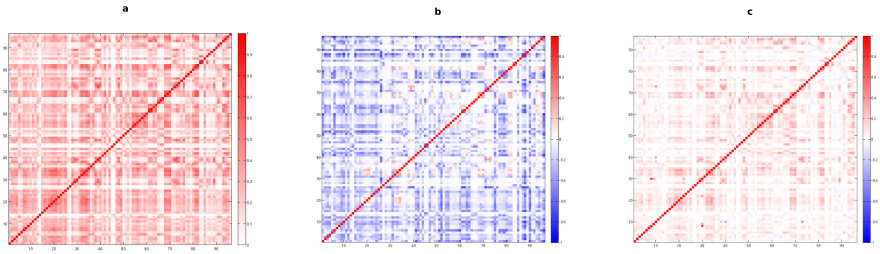


Figure 1.3: **Analysis of the weighted multiplexity between layers of the World Trade Multiplex in 2011.** Color-coded matrices with entries given by $m_w^{\alpha\beta}$ (a), $\mu_{WRG}^{\alpha\beta}$ (b) and $\mu_{WCM}^{\alpha\beta}$ (c) for any pair of layers (commodities).

### 1.3.2 Weighted analysis

Since the International Trade Network is represented by a weighted multiplex, the analysis of weighted overlaps between layers of that system can be performed, in order to obtain more refined information about the dependencies between different classes of commodities. We should indeed point out that, for the World Trade Web, while the binary overlaps provided by (1.2) only supply information about the dependencies between the topologies of the various layers representing trade in different commodities, the weighted multiplexity defined in (1.3) is able to detect patterns of correlation between quantities of imported and exported classes of items. In this perspective, observing high correlations is therefore more unlikely. This is due, mathematically, to the functional form of the definition of the multiplexity given in (1.3), which is significantly dependent on the balance between weights of the corresponding links in different layers; such a property, therefore, tends to assign higher correlations to pairs of commodities characterized by similar global amount of trade, as we want.

In Figure 1.3(a) we show the color-coded matrix $\mathbf{M}_w$ associated to the raw values of weighted multiplexity as observed in the International Trade Network: clear dependencies between different layers are still present, but a comparison with its corresponding binary matrix $\mathbf{M}_b$(shown in Figure 1.1(a)) explicitly reveals that, while some pairs of layers are significantly overlapping, several pairs of commodities are now actually uncorrelated, as expected when the weights of the links are taken into account. In order to provide information about the relation between the observed dependencies between layers and the expected ones under a given benchmark, as a first estimate, we calculate $\mu_{WRG}^{\alpha\beta}$, therefore considering the corresponding Weighted Random Graph (WRG) as a reference for our real-world network. Our findings show, in Figure 1.3(b), a strongly uncorrelated behavior associated to most of the pairs of commodities, in contrast with our intuitive

expectations based on the results obtained in the binary case.

We then compare the observed multiplexity with its expected values under the Weighted Configuration Model (WCM). Results, shown in Figure 1.3(c), exhibit a completely different behavior with respect to Figure 1.3(b), thus highlighting once more the importance of taking into account the heterogeneity in the weight and degree distributions within the considered null model. Indeed, we observe that, exploiting this more suitable reference, several pairs are still correlated, even in the weighted case, some of them are actually uncorrelated, as expected by looking at the corresponding binary matrix (Figure 1.1(c)), and only a few, with respect to the Weighted Random Graph case, remain anti-correlated. In general, however, the dependencies between layers in the weighted case are less noticeable, as we can see from a comparison between the matrices shown in Figures 1.1(c) and 1.3(c).

### 1.3.3 Hubs distribution

The different behaviours observed for the two considered multiplexes can be, at least partly, explained in terms of distribution of the hubs across layers. As we show in Figure 1.4(a) and 1.4(b), generally any two layers of the World Trade Multiplex exhibit the same set of hubs (which in this particular case are represented by the richest and most industrialized countries). Indeed, the two network layers plotted in the Figure are, already from visual inspection, very similar to each other. This property produces a high dependence between layers, since the overlap is increased by the multiple presence of links in the various layers connecting nodes to the hubs.

It is possible to show that this hubs distribution, leading to the higher overlap between layers, is strongly correlated to the relation existing between the hidden variables $x_i$ associated to each node in the different layers (we provide further details about such variables in appendices). Indeed, as shown in Figure 1.4(c), for the considered pair of layers (but several pairs actually exhibit the same behaviour) such a trend can be clearly represented by a straight line, thus pointing out that nodes with higher $x_i$ in one layer (hence, with higher probability of establishing a link with any other node in that layer) generally also have higher $x_i$ in a different layer.

However, when the European Airport Network is considered, an opposite trend can be observed, thus a clear explanation of the small measured overlap applies; indeed, Figures 1.5(a) and 1.5(b) show that in this case the layers can be approximated to star-like graphs, with a single, largely connected hub and several other poorly connected nodes. Though, the hub is in general different for almost any considered layer, since each airline company is based on a different airport: in the considered pair of layers, hubs are represented by Rome - Fiumicino airport (FCO) for Alitalia and Amsterdam - Schiphol airport (AMS) for KLM. Such a property decreases significantly the overlap between layers, thus leading to the matrices previously shown in Figure 1.2.

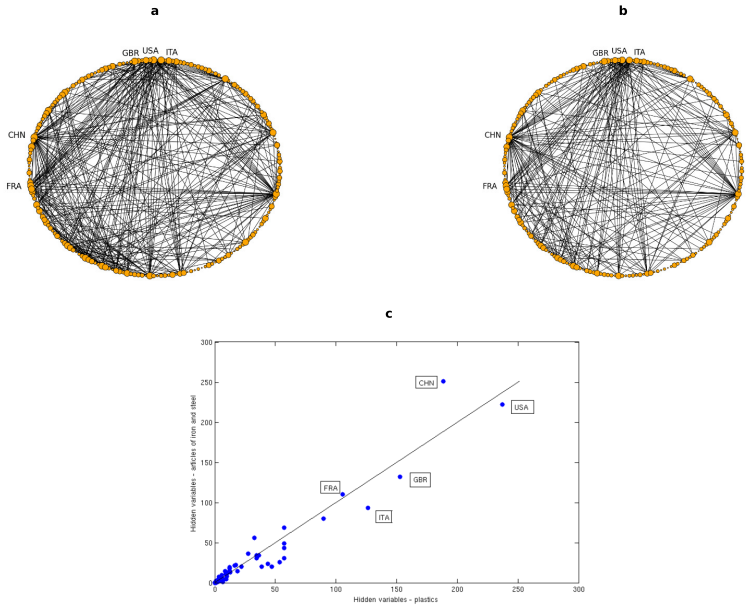


Figure 1.4: **Hubs distribution in the World Trade Multiplex.** Top panels: graphs representing two layers of the system, respectively those associated to trade in plastic (a) and articles of iron and steel (b); nodes represent trading countries; size of a node is proportional to its degree in that layer. Only links associated to a trade larger than 100 millions dollars are reported. Bottom panel: scatter plot of the hidden variables $x_i$ relative to each of the nodes for the same two layers; the black line represents the identity line.

Similar considerations can be done when looking at Figure 1.5(c), where the scatter plot of the hidden variables associated to the nodes in two different layers is shown. We observe that no linear trend can be inferred, since only the two hubs stand out from the bunch of the other airports (which are actually characterized by different values of $x_i$, even though this cannot be fully appreciated). It is anyway clear that the hub of one layer, characterized by the highest value $x_i$ (hence, with the highest probability of establishing a link with any other node in that layer) is a poorly connected node in a different layer, being characterized by a small value of $x_i$.

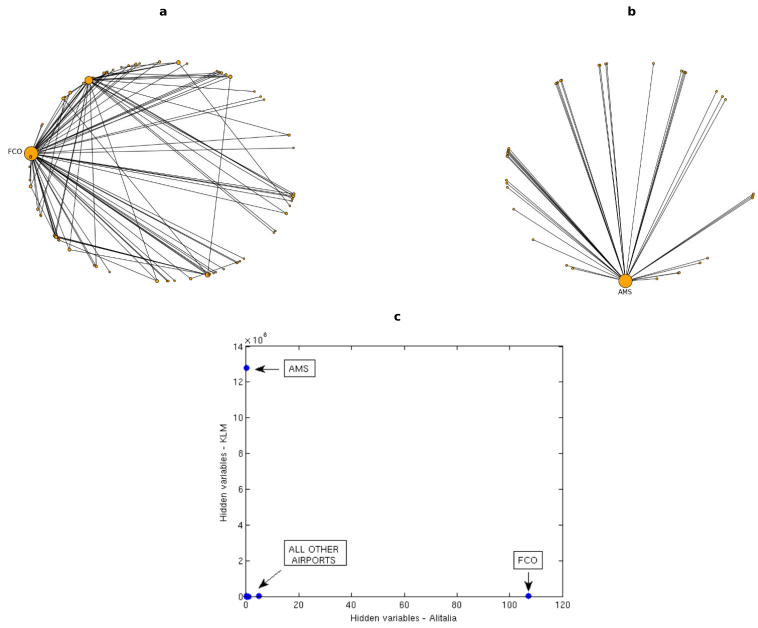


Figure 1.5: **Hubs distribution in the European Airport multiplex.** Top panels: graphs representing two layers of the system, respectively those associated to Alitalia airline (a) and KLM airline (b); nodes represent european airports; size of a node is proportional to its degree in that layer. All the observed links are reported. Bottom panel: scatter plot of the hidden variables $x_i$ relative to each of the nodes for the same two layers.

## 1.4 Discussion

In the last few years the multiplex approach has revealed itself as a useful framework to study several real-world systems characterized by elementary units linked by different kinds of connection. In this context, we have introduced new measures aiming at analyzing dependencies between layers of the network, both for binary and weighted multi-graphs. We showed that our measures of multiplexity are able to extract crucial information from both sparse and dense networks by testing it on different real-world multi-layer systems. We clearly found that a distinction can be done based on the degree of overlap between links in different layers. For instance, we showed that some multiplexes exhibit small overlap between links in different layers, since just a limited number of nodes are active in many layers, while most of them participate to one or few layers. However, for other systems, such as the World Trade Multiplex Network (WTM), most of the pairs of nodes are connected in several layers, so that such multiplexes exhibit large overlap

between layers. Furthermore, we found that the multiplexity can also provide interesting information about the distribution of hubs across the various layers; indeed, systems characterized by nodes having many connections in most of the layers, such as the WTM, tend to show higher values of raw binary multiplexity. On the other hand, in other networks exhibiting values of multiplexity for most of the pairs of layers close to 0, a node with a low degree in a given layer may represent a hub in a different layer: the European Airport Network is a clear prototype of such systems.

Our findings suggest that adopting proper null models for multi-level networks, enforcing constraints taking into account dependencies between layers, is required in order to suitably model such real-world systems.

Further research in this direction, including the studies reported in the following chapters, will hopefully provide a better understanding of the role of local constraints in real-world multi-level systems.

# Appendix

## 1.A Uncorrelated null models for multi-layer networks

We define the multiplex $\overrightarrow{G} = (G^1, G^2, \ldots, G^M)$ as the superposition of $M$ layers $G^\alpha$ ($\alpha = 1, 2, \ldots, M$), each of them represented by a (possibly weighted) network sharing the same set of $N$ nodes with the other ones, although we do not require that all the vertices are active in each layer. Therefore, multiplex ensembles can be defined by associating a probability $P(\overrightarrow{G})$ to each multi-network, so that the entropy $S$ of the ensemble is given by:

$$S = -\sum_{\overrightarrow{G}} P(\overrightarrow{G}) \ln P(\overrightarrow{G}) \tag{1.7}$$

It is then possible to design null models for multi-level networks by maximizing such an entropy after the enforcement of proper constraints. In this context, previous works, mentioned in the main text, introduced the concepts of correlated and uncorrelated multiplex ensembles, based on the possibility to introduce correlations between layers within the null models. In particular, for an uncorrelated ensemble the probability of a given multiplex can be factorized into the probabilities of each single-layer network $G^\alpha$ belonging to that multiplex, as the links in any two layers $\alpha$ and $\beta$ are uncorrelated; thus, it is given by:

$$P(\overrightarrow{G}) = \prod_{\alpha=1}^{M} P^\alpha(G^\alpha) \tag{1.8}$$

Instead, if we want to take into account correlations between layers, the previous relation (1.8) does not hold.

As stated in the main text, since our purpose is precisely that of measuring such correlations, we are going to consider the former type of ensemble, in order to define a null model for the real system so that it is possible to compare the observed correlations with reference models where the overlap between layers is actually randomized and, at the same time, important properties of the real network are preserved.

In this perspective, therefore, the definition of proper null models for the considered multiplex reduces to the definition of an indipendent null model for any layer of the system. In order to do this, we take advantage of the concept of canonical network ensemble, or exponential random graph, i.e. the randomized family of graphs satisfying a set of constraints on average. In this context the resulting randomized graph preserves only part of the topology of the considered real-world network and is entirely random otherwise, thus it can be employed as a proper reference model.

However, fitting such previously defined models to real datasets is hard, since it is usually computationally demanding as it requires the generation of many randomized networks whose properties of interest have to be measured. In this perspective, we make use of a fast and completely analytical maximum-entropy method, combined with the maximization of the likelihood function, which provides the exact probabilities of occurrence of random graphs with the same average constraints as the real network. From such probabilities it is then possible to compute the expectation values of the properties we are interested in, such as the average link probability or the average weight associated to the link established between any two nodes. This procedure is general enough to be applied to any network, including the denser ones, and does not require the sampling of the configuration space in order to compute average values of the quantities of interest. While the adoption of such a method is not strictly required when dealing with global constraints like the total number of links observed in a network, it becomes crucial when facing the problem of enforcing local constraints such as the degree sequence or the strength sequence.

Indeed, so far the most widely used graph null model has been represented by the Random Graph (RG), which enforces on average as constraint the expected number of links in the network. Such model, therefore, provides a unique expected probability $p^\alpha$ that a link between any two nodes is established in layer $\alpha$: however, as we said, such a reference model completely discards any kind of heterogeneity in the degree distributions of the layers, resulting in graphs where each node has on average the same number of connections, inconsistently with the observed real networks. Thus, the probability of connection between any two nodes in layer $\alpha$ is uniformly given by:

$$p^\alpha = \frac{L^\alpha}{N(N-1)/2} \tag{1.9}$$

where $L^\alpha$ is the total number of links actually observed in layer $\alpha$:

$$L^\alpha = \sum_{i<j} a_{ij}^\alpha \tag{1.10}$$

and $a_{ij}^\alpha = 0, 1$ depending on the presence of the link between nodes $i$ and $j$ in layer $\alpha$.

Similar considerations apply to weighted networks and the related Weighted Random Graph (WRG), i.e. the straightforward extension of the previous Random Graph to weighted systems; in such a null model, the probability of having a link of weight $w$ between two nodes $i$ and $j$ is independent from the choice of the nodes, and it is given by the following geometric distribution:

$$P(w^\alpha) = (p^\alpha)^w (1 - p^\alpha) \tag{1.11}$$

where the maximum-likelihood method shows that the optimal value of the parameter $p^\alpha$ is given by:

$$p^\alpha = \frac{2W^\alpha}{N(N-1) + 2W^\alpha} \tag{1.12}$$

with $W^\alpha$ defined as the total weight observed in layer $\alpha$ ($w_{ij}^\alpha$ is the weight associated to the link between nodes $i$ and $j$ in the same layer):

$$W^\alpha = \sum_{i<j} w_{ij}^\alpha \tag{1.13}$$

Similarly to the corresponding binary random graph, also this kind of null models discards the simultaneous presence of nodes characterized by high and low values of the strengths (that is, by a high or low sum of the weights associated to links incident on that node).

To take into account the heterogeneity of the real-world networks within the null models, in the unweighted case we consider the Binary Configuration Model (BCM), i.e. the ensemble of networks satisfying on average a given degree sequence. Since we make use of the canonical ensembles, it is possible to obtain from the maximum-likelihood method each probability $p_{ij}^\alpha$ that nodes $i$ and $j$ are connected in layer $\alpha$ (notice that such value $p_{ij}^\alpha$ is basically the expectation value of $a_{ij}^\alpha$ under the chosen Configuration Model). Similarly, for weighted graphs the Weighted Configuration Model (WCM) can be defined: here, the enforced constraint is represented by the strength sequence as observed in the real-world network. In this view, the likelihood maximization provides the expectation value of each weight $w_{ij}^\alpha$ for any pair of nodes $i$ and $j$ as supplied by the Weighted Configuration Model. It is worth noticing that enforcing the degree sequence (respectively, the strength sequence in the weighted case) automatically leads to the design of a null model where also the total number of links (respectively, the total weight) of the network is preserved. In the following section, we will provide

equations generalizing equations (1.9) and (1.12), whose solution allows then to derive the analytical expression of the expected link probability $p_{ij}^{\alpha}$ and, in the weighted case, the expected link weight $w_{ij}^{\alpha}$. In order to do this, we make use of a set of $N$ auxiliary variables $x_i^{\alpha}$ for any layer $\alpha$, which are proportional to the probability of establishing a link between a given node $i$ and any other node (or, respectively for the weighted case, establishing a link characterized by a given weight), being therefore directly informative on the expected probabilities $p_{ij}^{\alpha}$ (or, respectively, the expected weights $w_{ij}^{\alpha}$).

## 1.B Maximum-likelihood method

We now briefly explain the maximum-likelihood method (more details about this technique can be found in the appendix associated to Chapter 2, where it is also extended to the directed case). In the binary case, when the observed degree sequence represents the property that we want to preserve (i.e., in the so-called configuration model), the method reduces to finding the solution to following set of $N$ coupled nonlinear equation, independently for each layer $\alpha = 1, 2, \ldots, M$:

$$\sum_{i<j} \frac{x_i^{\alpha} x_j^{\alpha}}{1 + x_i^{\alpha} x_j^{\alpha}} = k_i^{\alpha} \quad \forall i = 1, 2, \ldots, N \tag{1.14}$$

where $k_i^{\alpha}$ is the observed degree of node $i$ in layer $\alpha$ and the unknown variables of the equation are the so-called $N$ hidden variables associated to that layer.

Thus, the expected link probability $p_{ij}^{\alpha}$ is given by, for any pair of nodes $(i, j)$ in any layer $\alpha$:

$$p_{ij}^{\alpha} = \frac{x_i^{\alpha} x_j^{\alpha}}{1 + x_i^{\alpha} x_j^{\alpha}} \tag{1.15}$$

which is therefore the generalization of the expression (1.9) in the previous section. We can therefore see that such hidden variables $x_i^{\alpha}$ are proportional to the expected link probability $p_{ij}^{\alpha}$ in a given layer $\alpha$: a higher value of $x_i^{\alpha}$ will correspond to a higher expected probability of observing a link between $i$ and any other node $j \neq i$, and vice-versa.

Similarly, for weighted multiplexes, we can enforce the strength sequence observed in a real network on a network ensemble, thus designing a proper null model where the strength sequence of the considered real-world network is preserved, while the other properties are randomized. In this context, the maximum-likelihood method for weighted graphs reduces to solving a set of $N$ coupled nonlinear equations. For any node $i$ in any layer $\alpha$, we have:

$$\sum_{i<j} \frac{x_i^{\alpha} x_j^{\alpha}}{1 - x_i^{\alpha} x_j^{\alpha}} = s_i^{\alpha} \tag{1.16}$$

where $s_i^\alpha$ is the observed strength of node $i$ in layer $\alpha$ and the unknown variables of the equation are, again, the $N$ hidden variables associated to the considered layer.

Thus, the expected link weight $w_{ij}^\alpha$ is given by, for any pair of nodes $(i, j)$:

$$w_{ij}^\alpha = \frac{x_i^\alpha x_j^\alpha}{1 - x_i^\alpha x_j^\alpha} \tag{1.17}$$

hence generalizing the corresponding equation (1.12). In this case, the computed hidden variables $x_i^\alpha$ are proportional to the expected link weight $w_{ij}^\alpha$ in a given layer $\alpha$; a higher value of $x_i^\alpha$ will therefore correspond to a higher expected link weight between $i$ and any other node $j \neq i$, and vice-versa.

We can now derive the expression for the expectation values of the binary and weighted multiplexity defined in the main text.

## 1.C Binary multiplexity

When the unweighted networks are considered we have defined the "absolute" binary multiplexity between any two layers $\alpha$ and $\beta$ as:

$$m_b^{\alpha\beta} = \frac{2\sum_{i<j} \min\{a_{ij}^\alpha, a_{ij}^\beta\}}{L^\alpha + L^\beta} \tag{1.18}$$

with the previously introduced notation.

As we said, this quantity is informative only after a comparison with the value of binary multiplexity obtained when considering a null model. We have therefore introduced the following transformed or rescaled quantity:

$$\mu_b^{\alpha\beta} = \frac{m_b^{\alpha\beta} - \langle m_b^{\alpha\beta}\rangle}{1 - \langle m_b^{\alpha\beta}\rangle} \tag{1.19}$$

where $m_b^{\alpha\beta}$ is the value measured for the observed real-world multiplex and $\langle m_b^{\alpha\beta}\rangle$ is the value expected under the chosen null model. We will show in the next section that, when the Random Graph is considered as a null model, the previous quantity (1.19) is actually the correlation coefficient between the entries of the adjacency matrix referred to any two layers $\alpha$ and $\beta$ of a multi-level graph.

We should point out that the raw intra-layer multiplexity $m_b^{\alpha\alpha}$ always leads to a measured value equal to 1, representing complete similarity between any layer and itself. However, the rescaled intra-layer multiplexity $\mu_{BCM}^{\alpha\alpha}$ actually leads to an indeterminate value; therefore, we choose to set this value by construction equal to 1 too, for sake of clarity.

In order to compute $\mu_b^{\alpha\beta}$ we should then calculate the expected multiplexity under the chosen null model, that is:

$$\langle m_b^{\alpha\beta}\rangle = \frac{2\sum_{i<j}\langle \min\{a_{ij}^\alpha, a_{ij}^\beta\}\rangle}{\langle L^\alpha\rangle + \langle L^\beta\rangle} \tag{1.20}$$

However, since both the considered null models preserve the average number of links in each layer as constraint, we have just to evaluate the analytical expression for the expected value of the minimum of two variables. In the unweighted case, this is easy because it reduces to the evaluation of the expected minimum between two indipendent, binary variables. In particular, when the Configuration Model is considered (the extension to the Random Graph is straightforward), the probability that a link exists between nodes $i$ and $j$ is given by the mass probability function of a Bernoulli-distributed variable:

$$P(a_{ij}^{\alpha}) = p_{ij}^{a_{ij}}(1-p_{ij})^{(1-a_{ij})} \tag{1.21}$$

Therefore, we have for the configuration model:

$$\begin{aligned}
\langle \min\{a_{ij}^{\alpha}, a_{ij}^{\beta}\}\rangle_{BCM} &= \sum_{a_{ij}^{\alpha}, a_{ij}^{\beta}} \min\{a_{ij}^{\alpha}, a_{ij}^{\beta}\} P\left(\min\{a_{ij}^{\alpha}, a_{ij}^{\beta}\}\right) = \\
&= 0 \cdot P\left(\min\{a_{ij}^{\alpha}, a_{ij}^{\beta}\} = 0\right) + 1 \cdot P\left(\min\{a_{ij}^{\alpha}, a_{ij}^{\beta}\} = 1\right) = \\
&= P\left(\min\{a_{ij}^{\alpha}, a_{ij}^{\beta}\} = 1\right) = \\
&= P\left(a_{ij}^{\alpha} = 1\right) P\left(a_{ij}^{\beta} = 1\right) = \\
&= p_{ij}^{\alpha} p_{ij}^{\beta}
\end{aligned} \tag{1.22}$$

and similarly for the Random Graph:

$$\langle \min\{a_{ij}^{\alpha}, a_{ij}^{\beta}\}\rangle_{RG} = p^{\alpha} p^{\beta} \tag{1.23}$$

where we define $p^{\alpha}$ as the fraction of links actually present in that layer, as we have already done before:

$$p^{\alpha} = \frac{L^{\alpha}}{N(N-1)/2} \tag{1.24}$$

It is now possible to compute the analytical expression for the rescaled multiplexity. We obtain for the Random Graph:

$$\mu_{RG}^{\alpha\beta} = \frac{2\sum_{i<j}\left(\min\{a_{ij}^{\alpha}, a_{ij}^{\beta}\} - p^{\alpha}p^{\beta}\right)}{\sum_{i<j}\left(a_{ij}^{\alpha} + a_{ij}^{\beta} - 2p^{\alpha}p^{\beta}\right)} \tag{1.25}$$

and for the Binary Configuration Model:

$$\mu_{BCM}^{\alpha\beta} = \frac{2\sum_{i<j}\left(\min\{a_{ij}^{\alpha}, a_{ij}^{\beta}\} - p_{ij}^{\alpha}p_{ij}^{\beta}\right)}{\sum_{i<j}\left(a_{ij}^{\alpha} + a_{ij}^{\beta} - 2p_{ij}^{\alpha}p_{ij}^{\beta}\right)} \tag{1.26}$$

### 1.C.1 Binary multiplexity: z-scores

As we have already said, such rescaled quantities provide proper information about the similarity between layers of a multiplex, by evaluating the dependencies measured in a real network with respect to what we would expect, on average, for an ensemble of multi-level networks sharing only some of the topological properties of the observed one. However, we cannot understand, from the obtained values of multiplexity itself, whether the observed value of $m_b^{\alpha\beta}$ is actually compatible with the expected one, as $\mu_{BCM}^{\alpha\beta}$ (and the correspondig value related to the Random Graph) does not provide any information about the standard deviation associated to the expected value of multiplexity.

In order to solve this issue, we introduce the z-score associated to the previously defined multiplexity:

$$z\left[m_b^{\alpha\beta}\right] = \frac{m_b^{\alpha\beta} - \langle m_b^{\alpha\beta}\rangle}{\sigma\left[m_b^{\alpha\beta}\right]} \tag{1.27}$$

where $m_b^{\alpha\beta}$ is the measured multiplexity between a given pair of layers on the real-world network, $\langle m_b^{\alpha\beta}\rangle$ is the value expected under the chosen null model and $\sigma[m_b^{\alpha\beta}]$ is the related standard deviation. The z-score, therefore, shows by how many standard deviations the observed value of multiplexity differs with respect to the expected one for any pair of layers. In particular, in the binary case such a quantity becomes:

$$z\left[m_b^{\alpha\beta}\right] = \frac{\sum_{i<j}\min\{a_{ij}^{\alpha}, a_{ij}^{\beta}\} - \sum_{i<j}\langle min\{a_{ij}^{\alpha}, a_{ij}^{\beta}\}\rangle}{\sigma\left[\sum_{i<j}\min\{a_{ij}^{\alpha}, a_{ij}^{\beta}\}\right]} \tag{1.28}$$

Interestingly, not only the expected value, but even the standard deviation can be calculated analytically. Indeed:

$$\sigma^2\left[\min\{a_{ij}^{\alpha}, a_{ij}^{\beta}\}\right] = \langle\min^2\{a_{ij}^{\alpha}, a_{ij}^{\beta}\}\rangle - \langle\min\{a_{ij}^{\alpha}, a_{ij}^{\beta}\}\rangle^2 \tag{1.29}$$

Exploiting again the binary character of the two indipendent variables $a_{ij}^{\alpha}$ and $a_{ij}^{\beta}$, the expected value of the square of the minimum becomes for the Configuration Model:

$$\begin{aligned}
\langle\min^2\{a_{ij}^{\alpha}, a_{ij}^{\beta}\}\rangle_{BCM} &= \sum_{a_{ij}^{\alpha}, a_{ij}^{\beta}} \min^2\{a_{ij}^{\alpha}, a_{ij}^{\beta}\} P\left(\min\{a_{ij}^{\alpha}, a_{ij}^{\beta}\}\right) = \\
&= 0\cdot P\left(\min\{a_{ij}^{\alpha}, a_{ij}^{\beta}\} = 0\right) + 1\cdot P\left(\min\{a_{ij}^{\alpha}, a_{ij}^{\beta}\} = 1\right) = \\
&= P\left(\min\{a_{ij}^{\alpha}, a_{ij}^{\beta}\} = 1\right) = \\
&= P\left(a_{ij}^{\alpha} = 1\right) P\left(a_{ij}^{\beta} = 1\right) = \\
&= p_{ij}^{\alpha} p_{ij}^{\beta}
\end{aligned} \tag{1.30}$$

Therefore, the standard deviation, required in order to evaluate the z-score associated to the multiplexity, is given by:

$$\sigma\left[\sum_{i<j}\min\{a_{ij}^{\alpha},a_{ij}^{\beta}\}\right]=\sqrt{\sum_{i<j}\left[p_{ij}^{\alpha}p_{ij}^{\beta}-\left(p_{ij}^{\alpha}p_{ij}^{\beta}\right)^{2}\right]} \tag{1.31}$$

The analytical value of the z-score related to the binary multiplexity, when the Configuration Model is taken into account, is then:

$$z_{BCM}^{\alpha\beta}=\frac{\sum_{i<j}\min\{a_{ij}^{\alpha},a_{ij}^{\beta}\}-\sum_{i<j}p_{ij}^{\alpha}p_{ij}^{\beta}}{\sqrt{\sum_{i<j}\left[p_{ij}^{\alpha}p_{ij}^{\beta}-\left(p_{ij}^{\alpha}p_{ij}^{\beta}\right)^{2}\right]}} \tag{1.32}$$

Extending such results to the Random Graph is immediate, since everything reduces to a change in the definition of the probability of observing a link between any given pair of nodes in each layer. Hence, the z-score associated to the binary multiplexity according to the binary Random Graph is given by:

$$z_{RG}^{\alpha\beta}=\frac{\sum_{i<j}\min\{a_{ij}^{\alpha},a_{ij}^{\beta}\}-\sum_{i<j}p^{\alpha}p^{\beta}}{\sqrt{\sum_{i<j}\left[p^{\alpha}p^{\beta}-\left(p^{\alpha}p^{\beta}\right)^{2}\right]}} \tag{1.33}$$

where we used the previous definitions for $p^{\alpha}$ and $p^{\beta}$.

We should point out that such z-scores should in principle be defined only if the associated property (in this case, $\mu_{BCM}^{\alpha\beta}$) is normally distributed; nevertheless, even if such assumption does not occur, they provide important information about the consistency between observed and randomized values. It is worth saying that these z-scores provide a different kind of information with respect to the previous multiplexities. Mathematically, the only correlation between, for example, $\mu_{BCM}^{\alpha\beta}$ and the corresponding $z_{BCM}^{\alpha\beta}$ is the sign concordance; furthermore, the z-score is useful in order to understand whether, for instance, values of multiplexity close to 0 are actually comparable with 0, so that we can consider those two layers as uncorrelated, or they are instead significantly unexpected, although very small. In this perspective, we should not expect a particular relation between such two variables $\mu_{BCM}^{\alpha\beta}$ and $z_{BCM}^{\alpha\beta}$ (or, respectively, $\mu_{RG}^{\alpha\beta}$ and $z_{RG}^{\alpha\beta}$).

### 1.C.2 Relationship with the correlation coefficient

A possible definition of correlation between layers of a multiplex builds on the standard correlation coefficient:

$$Corr\{a_{ij}^{\alpha},a_{ij}^{\beta}\}=\frac{\langle a_{ij}^{\alpha}a_{ij}^{\beta}\rangle-\langle a_{ij}^{\alpha}\rangle\langle a_{ij}^{\beta}\rangle}{\sigma_{\alpha}\sigma_{\beta}} \tag{1.34}$$

Hence, a value of correlation equal to 0 represents a pair of uncorrelated layers only if the probability distributions of $a_{ij}^{\alpha}$ and $a_{ij}^{\beta}$ are independent from the chosen node, that is, if all the edges in a certain layer are statistically equivalent. However, this leads to a probability of establishing a given link which is common to each pair of nodes, and this is the assumption behind the Random Graph.

In this context, it is then possible to show that, when the Binary Random Graph is taken into consideration, our novel measure of multiplexity can be reduced to the usual definition of correlation coefficient. Indeed, we have:

$$\begin{aligned}\langle a_{ij}^{\alpha} a_{ij}^{\beta} \rangle &= \frac{2\sum_{i<j} a_{ij}^{\alpha} a_{ij}^{\beta}}{N(N-1)} = \\ &= \frac{2\sum_{i<j} \min\{a_{ij}^{\alpha}, a_{ij}^{\beta}\}}{L^{\alpha}+L^{\beta}} \frac{L^{\alpha}+L^{\beta}}{N(N-1)} = \\ &= m_b^{\alpha\beta} \frac{L^{\alpha}+L^{\beta}}{N(N-1)} \end{aligned} \tag{1.35}$$

Moreover, the average value of $a_{ij}^{\alpha}$ over all the pairs of nodes in layer $\alpha$ is given by:

$$\langle a_{ij}^{\alpha} \rangle = \frac{2L^{\alpha}}{N(N-1)} \tag{1.36}$$

and similarly for layer $\beta$:

$$\langle a_{ij}^{\beta} \rangle = \frac{2L^{\beta}}{N(N-1)} \tag{1.37}$$

Hence,

$$\langle a_{ij}^{\alpha} \rangle \langle a_{ij}^{\beta} \rangle = \frac{4L^{\alpha}L^{\beta}}{N^2(N-1)^2} \tag{1.38}$$

On the contrary, the expected value of multiplexity under random graph is given by:

$$\begin{aligned}\langle m_b^{\alpha\beta} \rangle &= \frac{2\sum_{i<j} p^{\alpha} p^{\beta}}{L^{\alpha}+L^{\beta}} = \\ &= \frac{N(N-1)}{L^{\alpha}+L^{\beta}} \frac{2L^{\alpha}}{N(N-1)} \frac{2L^{\beta}}{N(N-1)} = \\ &= \frac{1}{N(N-1)} \frac{4L^{\alpha}L^{\beta}}{L^{\alpha}+L^{\beta}} \end{aligned} \tag{1.39}$$

There is therefore a direct relation between $\langle a_{ij}^{\alpha} \rangle \langle a_{ij}^{\beta} \rangle$ and $\langle m_b^{\alpha\beta} \rangle$:

$$\begin{aligned}\langle a_{ij}^{\alpha} \rangle \langle a_{ij}^{\beta} \rangle &= \frac{4L^{\alpha}L^{\beta}}{N^2(N-1)^2} = \\ &= \langle m_b^{\alpha\beta} \rangle \frac{L^{\alpha}+L^{\beta}}{N(N-1)} \end{aligned} \tag{1.40}$$

Furthermore, we need to derive the expression for the standard deviation $\sigma_\alpha$ and $\sigma_\beta$:

$$\begin{aligned}\sigma_\alpha &= \sqrt{\langle \left(a_{ij}^\alpha\right)^2\rangle - \langle a_{ij}^\alpha\rangle^2} = \\ &= \sqrt{\langle a_{ij}^\alpha\rangle \left(1 - \langle a_{ij}^\alpha\right)} = \\ &= \sqrt{\frac{2L^\alpha}{N(N-1)}\left[1 - \frac{2L^\alpha}{N(N-1)}\right]}\end{aligned} \tag{1.41}$$

and analogously for $\beta$. Hence, the correlation coefficient between $a_{ij}^\alpha$ and $a_{ij}^\beta$ is given by:

$$\begin{aligned}Corr\{a_{ij}^\alpha, a_{ij}^\beta\} &= \frac{\frac{L^\alpha+L^\beta}{N(N-1)} m_b^{\alpha\beta} - \frac{L^\alpha+L^\beta}{N(N-1)}\langle m_b^{\alpha\beta}\rangle}{\frac{2}{N(N-1)}\sqrt{L^\alpha L^\beta\left(1-\frac{2L^\alpha}{N(N-1)}\right)\left(1-\frac{2L^\beta}{N(N-1)}\right)}} \\ &= \frac{\left(L^\alpha + L^\beta\right)\left(m_b^{\alpha\beta} - \langle m_b^{\alpha\beta}\rangle\right)}{2\sqrt{L^\alpha L^\beta\left(1-\frac{2L^\alpha}{N(N-1)}\right)\left(1-\frac{2L^\beta}{N(N-1)}\right)}}\end{aligned} \tag{1.42}$$

It is therefore clear that, apart from a different normalization factor (depending on $L^\alpha$ and $L^\beta$), our definition of binary rescaled multiplexity, when the Random Graph is considered as null model, reduces to the usual correlation coefficient (1.34).

However, such a property does not hold when a different reference model, such as the Configuration Model, is considered.

## 1.D Weighted multiplexity

In the main text, we have also extended the previous definitions to weighted multiplex networks. We have defined the "absolute" weighted multiplexity as:

$$m_w^{\alpha\beta} = \frac{2\sum_{i<j}\min\{w_{ij}^\alpha, w_{ij}^\beta\}}{W^\alpha + W^\beta} \tag{1.43}$$

where $w_{ij}^\alpha$ represents the weight of the link between nodes $i$ and $j$ in layer $\alpha$ and $W^\alpha$ is the total weight related to the links in that layer.

Furthermore, we have defined the following transformed or rescaled quantity:

$$\mu_w^{\alpha\beta} = \frac{m_w^{\alpha\beta} - \langle m_w^{\alpha\beta}\rangle}{1 - \langle m_w^{\alpha\beta}\rangle} \tag{1.44}$$

where $\langle m_w^{\alpha\beta}\rangle$ is the value measured for the observed real-world network and $\langle m_w^{\alpha\beta}\rangle$ is the value expected under the considered reference model. Again, the sign of

$\mu_w^{\alpha\beta}$ is then directly informative about the weighted dependency existing between layers.

In this context, the expected value of weighted multiplexity is given by:

$$\langle m_w^{\alpha\beta} \rangle = \frac{2\sum_{i<j}\langle \min\{w_{ij}^{\alpha}, w_{ij}^{\beta}\}\rangle}{\langle W^{\alpha}\rangle + \langle W^{\beta}\rangle} \tag{1.45}$$

However, since both the Weighted Random Graph and the Weighted Configuration Model preserve the average total weight associated to the links in each layer as constraint, also in this case we just need to evaluate the analytical expression for the expected value of the minimum of two variables; the only difference with respect to the binary description is related to a change in the underlying probability distribution.

Indeed, in the weighted case, when the Weighted Configuration Model is considered (again, the extension to the Weighted Random Graph is straightforward) such variables are distributed according to a geometrical distribution:

$$P(w_{ij}^{\alpha}) = p_{ij}^{w_{ij}^{\alpha}}(1 - p_{ij}^{\alpha}) \tag{1.46}$$

In order to quantify such an expectation value, we exploit the cumulative distribution of the minimum between the considered variables:

$$\begin{aligned} P\left(\min\{w_{ij}^{\alpha}, w_{ij}^{\beta}\} \geq w\right) &= P\left(w_{ij}^{\alpha} \geq w\right) P\left(w_{ij}^{\beta} \geq w\right) = \\ &= \left(p_{ij}^{\alpha} p_{ij}^{\beta}\right)^{w} \end{aligned} \tag{1.47}$$

Thus, the expected minimum, under Weighted Configuration Model, becomes:

$$\begin{aligned} \langle \min\{w_{ij}^{\alpha}, w_{ij}^{\beta}\}\rangle_{WCM} &= \sum_{w'} w'[P\left(\min\{w_{ij}^{\alpha}, w_{ij}^{\beta}\} \geq w'\right) + \\ &- P\left(\min\{w_{ij}^{\alpha}, w_{ij}^{\beta}\} \geq w' + 1\right)] = \\ &= \sum_{w'} w' \left[\left(p_{ij}^{\alpha} p_{ij}^{\beta}\right)^{w'} - \left(p_{ij}^{\alpha} p_{ij}^{\beta}\right)^{w'+1}\right] = \\ &= \frac{p_{ij}^{\alpha} p_{ij}^{\beta}}{1 - p_{ij}^{\alpha} p_{ij}^{\beta}} \end{aligned} \tag{1.48}$$

and, for the Weighted Random Graph:

$$\langle \min\{w_{ij}^{\alpha}, w_{ij}^{\beta}\}\rangle_{WRG} = \frac{p^{\alpha} p^{\beta}}{1 - p^{\alpha} p^{\beta}} \tag{1.49}$$

where we define $p^{\alpha}$, according to the likelihood maximization, as:

$$p^{\alpha} = \frac{W^{\alpha}}{W^{\alpha} + N(N-1)/2}, \tag{1.50}$$

We can now compute the analytical expression for the rescaled multiplexity, according to both the chosen null models. We obtain for the Weighted Random Graph (WRG):

$$\mu^{\alpha\beta}_{WRG} = \frac{2\sum_{i<j}\left(\min\{w^{\alpha}_{ij}, w^{\beta}_{ij}\} - \frac{p^{\alpha}p^{\beta}}{1-p^{\alpha}p^{\beta}}\right)}{\sum_{i<j}\left(w^{\alpha}_{ij} + w^{\beta}_{ij} - 2\frac{p^{\alpha}p^{\beta}}{1-p^{\alpha}p^{\beta}}\right)} \tag{1.51}$$

and for the Weighted Configuration Model (WCM):

$$\mu^{\alpha\beta}_{WCM} = \frac{2\sum_{i<j}\left(\min\{w^{\alpha}_{ij}, w^{\beta}_{ij}\} - \frac{p^{\alpha}_{ij}p^{\beta}_{ij}}{1-p^{\alpha}_{ij}p^{\beta}_{ij}}\right)}{\sum_{i<j}\left(w^{\alpha}_{ij} + w^{\beta}_{ij} - 2\frac{p^{\alpha}_{ij}p^{\beta}_{ij}}{1-p^{\alpha}_{ij}p^{\beta}_{ij}}\right)} \tag{1.52}$$

with the previously defined notation.

### 1.D.1 Weighted multiplexity: z-scores

Furthermore, we can extend to the weighted case the analysis of the z-scores associated to the values of multiplexity as defined in (1.44). We can define it in the usual way:

$$z\left[m^{\alpha\beta}_{w}\right] = \frac{\sum_{i<j}\min\{w^{\alpha}_{ij}, w^{\beta}_{ij}\} - \sum_{i<j}\langle\min\{w^{\alpha}_{ij}, w^{\beta}_{ij}\}\rangle}{\sigma\left[\sum_{i<j}\min\{w^{\alpha}_{ij}, w^{\beta}_{ij}\}\right]} \tag{1.53}$$

Since:

$$\sigma^2\left[\min\{w^{\alpha}_{ij}, w^{\beta}_{ij}\}\right] = \langle\min^2\{w^{\alpha}_{ij}, w^{\beta}_{ij}\}\rangle - \langle\min\{w^{\alpha}_{ij}, w^{\beta}_{ij}\}\rangle^2 \tag{1.54}$$

we just have to compute the analytical expression for the expected value of the square of minimum bewteeen $w^{\alpha}_{ij}$ and $w^{\beta}_{ij}$. Then, following the same procedure adopted for (1.48) we find:

$$\begin{aligned}
\langle\min^2\{w^{\alpha}_{ij}, w^{\beta}_{ij}\}\rangle_{WCM} &= \sum_{w'}(w')^2\left[P\left(\min\{w^{\alpha}_{ij}, w^{\beta}_{ij}\} \geq w'\right) + \right. \\
&- \left. P\left(\min\{w^{\alpha}_{ij}, w^{\beta}_{ij}\} \geq w'+1\right)\right] = \\
&= \sum_{w'}(w')^2\left[\left(p^{\alpha}_{ij}p^{\beta}_{ij}\right)^{w'} - \left(p^{\alpha}_{ij}p^{\beta}_{ij}\right)^{w'+1}\right] = \\
&= \frac{p^{\alpha}_{ij}p^{\beta}_{ij} + \left(p^{\alpha}_{ij}p^{\beta}_{ij}\right)^2}{\left(1-p^{\alpha}_{ij}p^{\beta}_{ij}\right)^2}
\end{aligned} \tag{1.55}$$

and therefore the standard deviation is:

$$\sigma\left[\sum_{i<j}\min\{w_{ij}^{\alpha},w_{ij}^{\beta}\}\right]=\sqrt{\sum_{i<j}\left[\frac{p_{ij}^{\alpha}p_{ij}^{\beta}+\left(p_{ij}^{\alpha}p_{ij}^{\beta}\right)^{2}}{\left(1-p_{ij}^{\alpha}p_{ij}^{\beta}\right)^{2}}-\frac{\left(p_{ij}^{\alpha}p_{ij}^{\beta}\right)^{2}}{\left(1-p_{ij}^{\alpha}p_{ij}^{\beta}\right)^{2}}\right]} \tag{1.56}$$

Finally, the z-score associated to the weighted multiplexity under Weighted Configuration Model is therefore given by:

$$z_{WCM}^{\alpha\beta}=\frac{\sum_{i<j}\min\{w_{ij}^{\alpha},w_{ij}^{\beta}\}-\sum_{i<j}\frac{p_{ij}^{\alpha}p_{ij}^{\beta}}{1-p_{ij}^{\alpha}p_{ij}^{\beta}}}{\sqrt{\sum_{i<j}\frac{p_{ij}^{\alpha}p_{ij}^{\beta}}{\left(1-p_{ij}^{\alpha}p_{ij}^{\beta}\right)^{2}}}} \tag{1.57}$$

Analogously, we get:

$$z_{WRG}^{\alpha\beta}=\frac{\sum_{i<j}\min\{w_{ij}^{\alpha},w_{ij}^{\beta}\}-\sum_{i<j}\frac{p^{\alpha}p^{\beta}}{1-p^{\alpha}p^{\beta}}}{\sqrt{\sum_{i<j}\frac{p^{\alpha}p^{\beta}}{(1-p^{\alpha}p^{\beta})^{2}}}} \tag{1.58}$$

for the Weighted Random Graph, where we used the previous definitions for $p^{\alpha}$ and $p^{\beta}$.

## 1.E Additional results

As we stated in the main text, in order to have a better understanding of the correlations between layers, it is possible to implement a hierarchical clustering procedure starting from each of the aforementioned multiplexity matrices. However, we have to define a notion of distance between layers, starting from our notion of dependency. We can define a distance $d^{\alpha\beta}$ between any pair of commodities in the following way:

$$d^{\alpha\beta}=\sqrt{\frac{1-\mu_{BCM}^{\alpha\beta}}{2}}. \tag{1.59}$$

where we chose to consider, for instance, the transformed multiplexity under Binary Configuration Model. Hence, the maximum possible distance $d^{\alpha\beta}$ between any two layers is 1 (when layers $\alpha$ and $\beta$ show multiplexity $\mu_{BCM}^{\alpha\beta}=1$), while the minimum one is 0 (corresponding to $\mu_{BCM}^{\alpha\beta}=-1$). We can therefore represent the layers of the multiplex as the leaves of a taxonomic tree, where highly correlated communities meet at a branching point which is closer to baseline level. In Figure 1.6 we show the dendrogram obtained by applying the Average Linkage Clustering Algorithm to the matrix representing values of multiplexity $\mu_{BCM}^{\alpha\beta}$ for the World Trade Multiplex (WTM). We can see that some groups of similar commodities are

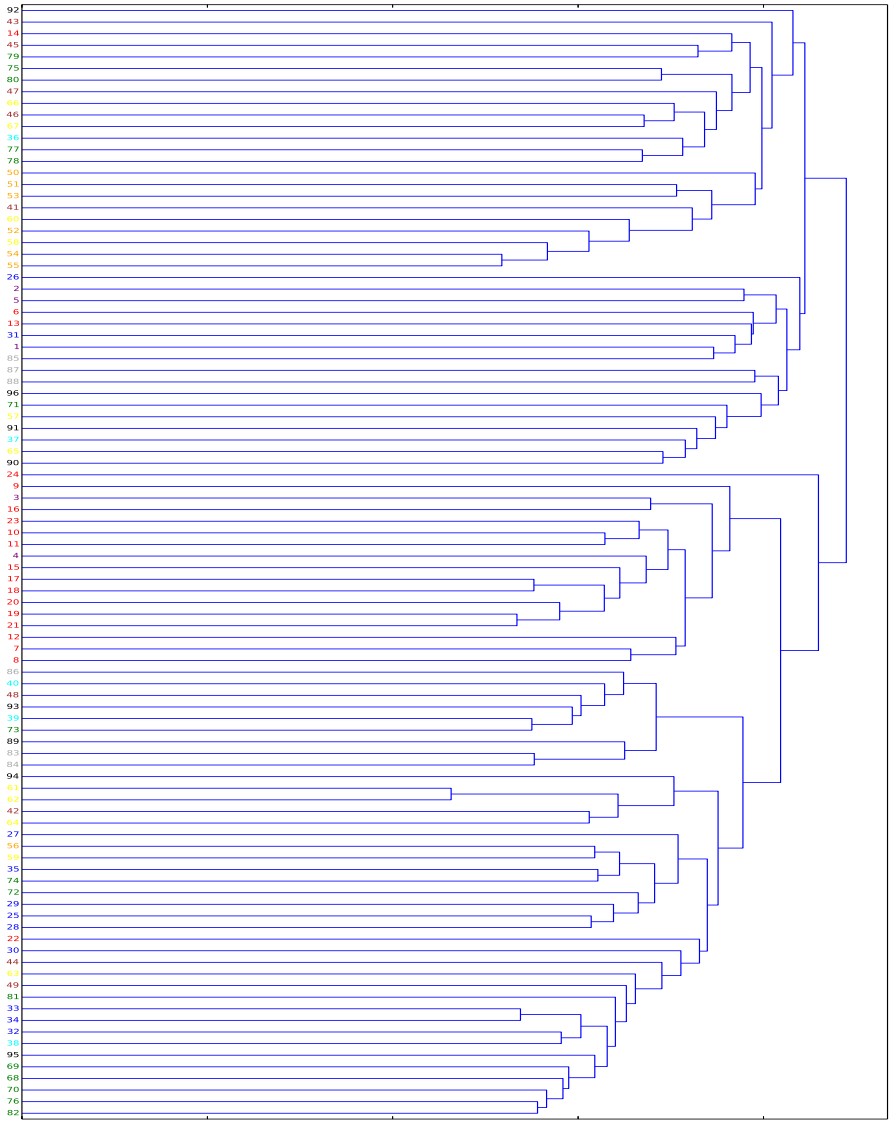

Figure 1.6: **Dendrogram of commodities traded in 2011 in the WTM as obtained applying the Average Linkage Clustering Algorithm to the binary rescaled multiplexity $\mu^{\alpha\beta}_{BCM}$.** Colors of the leaves represent different classes of commodities, as reported in the last Section of this Appendix.

clearly visible (for instance, the group of edible commodities can be easily identified), while in other cases apparently distant commodities are grouped together, pointing out that some unexpected dependencies are present. The dendrogram reported in Figure 1.6 therefore represents a refinement of the taxonomic tree reported in previous studies, where the usual correlation coefficient was employed to define the dependency between layers. Similar dendrograms can be designed starting from the matrices representing values of $\mu_{RG}^{\alpha\beta}$ or weighted multiplexity $\mu_{WRG}^{\alpha\beta}$ and $\mu_{WCM}^{\alpha\beta}$.

Moreover, it is possible to perform the same analysis on the European Airport Network. However, a dendrogram in this case would not be meaningful, since most of the layers meet at a single root level, due to the very low correlation observed between them.

As we said, color-coded multiplexity matrices, as shown in the main text, are useful in order to detect the meaninful dependencies between layers in a multiplex, but they do not supply any information about the discrepancy of the observed values from the corresponding expected ones. Hence, the introduction of suitable z-scores associated to the previously defined quantities is required. Moreover, it is worth reminding that the information provided by (1.26) (respectively (1.25) for the Random Graph) is not necessarily connected to that supplied by (1.32) (respectively, (1.33)) Indeed, while the multiplexity by itself detects the degree of correlation between layers of a multi-level network, the corresponding z-scores reveal how significant those values actually are with respect to our expectations. In Figure 1.7(a) we show, for the World Trade Multiplex (WTM), the scatter

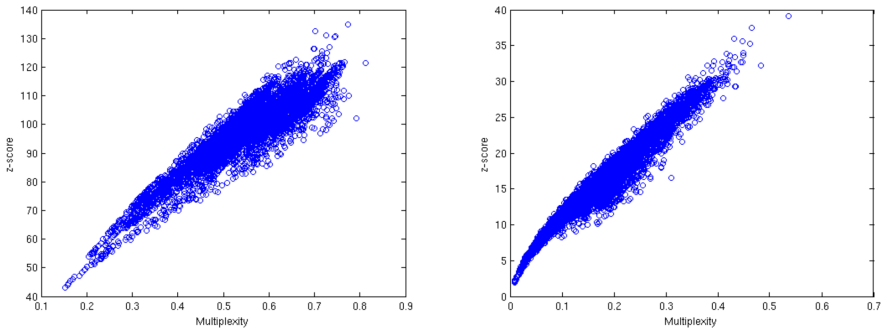


Figure 1.7: **Significance of the binary multiplexity values for the World Trade Multiplex.** Scatter plots of binary multiplexity values $\mu_b^{\alpha\beta}$ vs the corresponding z-score for each pair of layers, respectively for Random Graph (a) and Binary Configuration Model (b), for the WTM.

plot of the values of binary multiplexity versus the corresponding z-scores, after comparing the observed values with the expected ones under Random Graph. We show that observed very large values of z-scores reveal a high significance of

the previously obtained overlaps; such a consideration therefore points out that even the pairs of layers showing low (but positive) values of multiplexity cannot actually be considered as uncorrelated. Furthermore, a clear correlation between $\mu_{RG}^{\alpha\beta}$ and $z_{RG}^{\alpha\beta}$ can be observed, thus large values of binary multiplexity correspond to large z-scores, and vice-versa.

Similar considerations can be done when the Binary Configuration Model is considered as a benchmark. Indeed, as we show in Figure 1.7(b), a large correlation between $\mu_{BCM}^{\alpha\beta}$ and $z_{BCM}^{\alpha\beta}$ is still present when we consider the WTM; moreover, since almost all the z-scores are higher than the widely used critical value $z_{BCM}^{*} = 2$ (so that almost no pair of layers shows a multiplexity lying within 2 standard deviations form the expected value), we highlight that most of the pairs therefore exhibit unexpectedly high correlations with respect to the corresponding average value obtained when randomizing the real-world layers according to the Configuration Model, similarly to what we found before for the Random Graph.

However, if we look at the absolute values of such z-scores, we observe that the significance of the values of multiplexity under Random Graph ($\mu_{RG}^{\alpha\beta}$) is generally much higher than that measured under Binary Configuration Model ($\mu_{BCM}^{\alpha\beta}$). This property, which will still be true in the following Figures, is actually not surprising, since the Configuration Model enforces more constraints and therefore leads to higher similarity with the real network w.r.t the Random Graph.

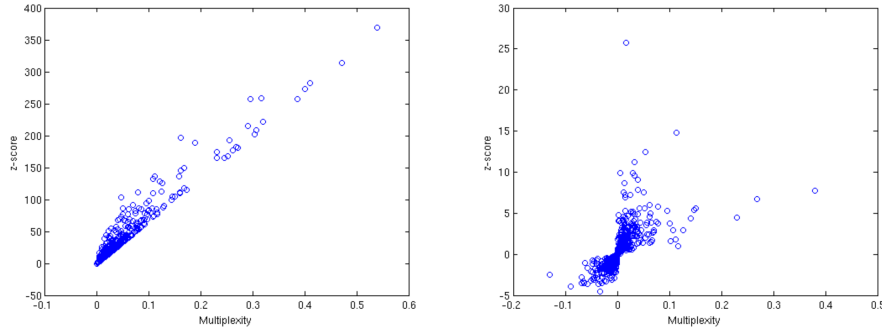


Figure 1.8: **Significance of the binary multiplexity values for the European Airport Network.** Scatter plots of binary multiplexity values $\mu_b^{\alpha\beta}$ vs the corresponding z-score for each pair of layers, respectively for Random Graph (a) and Binary Configuration Model (b).

A different trend can be observed when the European Airport Network is taken into account (Figure 1.8(a)). Indeed, it is still clear a high correlation between values of multiplexity and their respective z-scores when the Random Graph is considered. However, many z-scores associated to multiplexities close to 0, in this case, are now close to 0 themselves, therefore suggesting that many pairs of

layers (i.e. airline companies) may actually be anti-correlated rather than simply uncorrelated. In this case, the adoption of a more refined null model is then crucial in order to deeply understand the structural properties of such a system.

When the Binary Configuration Model is considered as benchmark, however, the analysis of the corresponding scatter plots dramatically changes. However, as we said, these results are strongly dependent on the considered network. Indeed, Figure 1.8(b) exhibits a completely different trend with respect, for instance, to the corresponding Figure 1.7(b) (related to the World Trade Multiplex): no correlation between $\mu^{\alpha\beta}_{BCM}$ and $z^{\alpha\beta}_{BCM}$ can be observed in this case, so that the same value of multiplexity can be either associated to a low z-score (thus being compatible with the expected value under the chosen Configuration Model) or to very high z-scores (hence unexpectedly different from the model's expectation). Moreover, Figure 1.8(b) clearly shows the sign-concordance existing between the multiplexity and the associated z-score that we pointed out in the previous Section. However, no other clear trend can be inferred from such a plot, therefore pointing out the importance of taking into account both the quantities ($\mu^{\alpha\beta}_{BCM}$ and $z^{\alpha\beta}_{BCM}$) in order to have a complete understanding of the correlations between layers of a multiplex.

Furthermore, we should highlight once more that, in terms of absolute z-scores values, the significance of the values of multiplexity under Random Graph ($\mu^{\alpha\beta}_{RG}$) is usually much higher than that observed after the comparison with the Configuration Model ($\mu^{\alpha\beta}_{BCM}$), as we have already found before for the WTM.

Similarly, we can analyze the patterns of correlations resulting from the z-scores associated to the weighted multiplexity, as defined in (1.58) and (1.57). In Figure 1.9(a) we show the relation between the values of weighted multiplexity for any pair of layers and the related z-score, computed with respected to the expected multiplexity according to the Weighted Random Graph. The sign concordance is still clear, but the correlation between $\mu^{\alpha\beta}_{WRG}$ and $z^{\alpha\beta}_{WRG}$ is much less sharp with respect to the corresponding binary case, especially for negative values of multiplexity.

Even more so, such a weak correlation between weighted multiplexity and the corresponding z-score completely disappears when the considered benchmark is the Weighted Configuration Model (Figure 1.9(b)): in this case the same value of $\mu^{\alpha\beta}_{WCM}$ may correspond to z-scores even characterized by different orders of magnitude, thus pointing out once more the importance of the introduction of a notion of standard deviation referred to the average $\langle \mu^{\alpha\beta}_{WCM} \rangle$. Indeed, the same value of observed multiplexity can actually be either extremely unexpected or in full agreement with the null model's prediction.

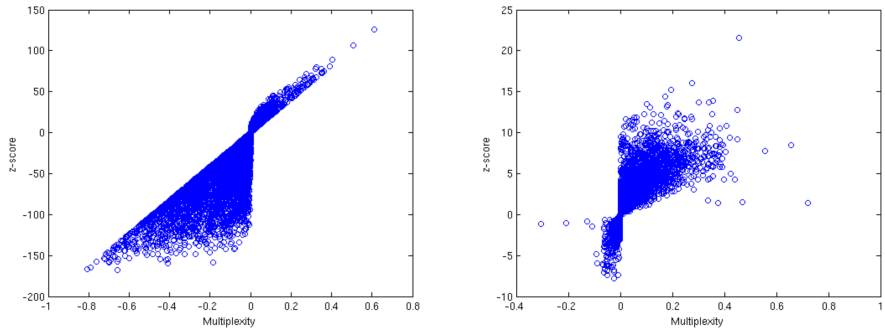


Figure 1.9: **Significance of the weighted multiplexity values for the World Trade Multiplex.** Scatter plots of weighted multiplexity values $\mu_w^{\alpha\beta}$ vs the corresponding z-scores for each pair of layers, respectively for Weighted Random Graph (a) and Weighted Configuration Model (b).

## 1.F International Trade Multiplex Network: list of layers

Throughout this thesis we meticulously analyze the World Trade Multiplex Network (WTM), as provided by the BACI database mentioned in the main text. The data provide information about import and export between $N = 207$ countries (we focus in particular on the year 2011) and turn out to have a straightforward representation in terms of multi-layered network; it is indeed possible to disaggregate the global trade between any two countries into the import and export in a given commodity, so that the global trade system can be thought of as the superposition of all the layers. The network is then composed by 207 countries and $M = 96$ different commodities, according to the standard international classification HS1996 (the list of commodities is reported below in Table 1.1). While the aggregated network shows a density higher than 55%, the various layers are characterized by densities from 6% (related to trade in silk) to 45% (for import-export of mechanical appliances and parts thereof). Such heterogeneity may suggest that a multiplex analysis is therefore required. Interestingly, in this case each of the layers is represented by a weighted network, where the weight associated to any link in a layer stands for the amount of money exchanged by a given pair of countries in that layer (i.e., commodity).

| | Commodity | |
|---|---|---|
| 01 | Live animals | ● |
| 02 | Meat and edible meat offal | ● |
| 03 | Fish, crustaceans and acquatic invertebrates | ● |
| 04 | Dairy produce; birs eggs; honey and other edible animal products | ● |
| 05 | Other products of animal origin | ● |
| 06 | Live trees, plants; bulbs, roots; cut flowers and ornamental foliage tea and spices | ● |
| 07 | Edible vegetables and certain roots and tubers | ● |
| 08 | Edible fruit and nuts; citrus fruit or melon peel | ● |
| 09 | Coffee, tea, mate and spices | ● |
| 10 | Cereals | ● |
| 11 | Milling products; malt; starch; inulin; wheat gluten | ● |
| 12 | Oil seeds and oleaginous fruits; miscellaneous grains, seeds and fruit; industrial or medicinal plants; straw and fodder | ● |
| 13 | Lac; gums, resins and other vegetable sap and extracts | ● |
| 14 | Vegetable plaiting materials and other vegetable products | ● |
| 15 | Animal, vegetable fats and oils, cleavage products, etc. | ● |
| 16 | Edible preparations of meat, fish, crustaceans, mollusks or other aquatic invertebrates | ● |
| 17 | Sugars and sugar confectionary | ● |
| 18 | Cocoa and cocoa preparations | ● |
| 19 | Preparations of cereals, flour, starch or milk; bakers wares | ● |
| 20 | Preparations of vegetables, fruit, nuts or other plant parts | ● |
| 21 | Miscellaneous edible preparations | ● |
| 22 | Beverages, spirits and vinegar | ● |
| 23 | Food industry residues and waste; prepared animal feed | ● |
| 24 | Tobacco and manufactured tobacco substitutes | ● |
| 25 | Salt; sulfur; earth and stone; lime and cement plaster | ● |
| 26 | Ores, slag and ash | ● |
| 27 | Mineral fuels, mineral oils and products of their distillation; bitumin substances; mineral wax | ● |
| 28 | Inorganic chemicals; organic or inorganic compounds of precious metals, of rare-earth metals, of radioactive elements or of isotopes | ● |

| | | |
|---|---|---|
| 29 | Organic chemicals | ● |
| 30 | Pharmaceutcal products | ● |
| 31 | Fertilizers | ● |
| 32 | Tanning or dyeing extracts; tannins and derivatives; dyes, pigments and coloring matter; paint and varnish; putty and other mastics; inks | ● |
| 33 | Essential oils and resinoids; perfumery, cosmetic or toilet preparations | ● |
| 34 | Soap; waxes; polish; candles; modeling pastes; dental preparations with basic of plaster | ● |
| 35 | Albuminoidal substances; modified starch; glues; enzymes | ● |
| 36 | Explosives; pyrotechnic products; matches; pyrophoric alloys; certain combustible preparations | ● |
| 37 | Photographic or cinematographic goods | ● |
| 38 | Miscellaneous chemical products | ● |
| 39 | Plastics and articles thereof | ● |
| 40 | Rubber and articles thereof | ● |
| 41 | Raw hides and skins (other than furskins) and leather | ● |
| 42 | Leather articles; saddlery and harness; travel goods, handbags and similar; articles of animal gut (not silkworm gut) | ● |
| 43 | Furskins and artificial fur; manufactures thereof | ● |
| 44 | Wood and articles of wood; wood charcoal | ● |
| 45 | Cork and articles of cork | ● |
| 46 | Manufactures of straw, esparto or other plaiting materials; basketware and wickerwork | ● |
| 47 | Pulp of wood or of other fibrous cellulosic material; waste and scrap of paper and paperboard | ● |
| 48 | Paper and paperboard and articles thereof; paper pulp articles | ● |
| 49 | Printed books, newspapers, pictures and other products of printing industry; manuscripts, typescripts | ● |
| 50 | Silk, including yarns and woven fabric thereof | ● |
| 51 | Wool and animal hair, including yarn and woven fabric | ● |
| 52 | Cotton, including yarn and woven fabric thereof | ● |
| 53 | Other vegetable textile fibers; paper yarn and woven fabrics of paper yarn | ● |
| 54 | Manmade filaments, including yarns and woven fabrics | ● |
| 55 | Manmade staple fibers, including yarns and woven fabrics | ● |

| | | |
|---|---|---|
| 56 | Wadding, felt and nonwovens; special yarns; twine, cordage, ropes and cables and article thereof | 🟠 |
| 57 | Carpets and other textile floor coverings | 🟠 |
| 58 | Special woven fabrics; tufted textile fabrics; lace; tapestries; trimmings; embroidery | 🟡 |
| 59 | Impregnated, coated, covered or laminated textile fabrics; textile articles for industrial use | 🟡 |
| 60 | Knitted or crocheted fabrics | 🟡 |
| 61 | Apparel articles and accessories, knitted or crocheted | 🟡 |
| 62 | Apparel articles and accessories, not knitted or crocheted | 🟡 |
| 63 | Other textile articles; needlecraft sets; worn clothing and worn textile articles; rags | 🟡 |
| 64 | Footwear, gaiters and the like and parts thereof | 🟡 |
| 65 | Headgear and parts thereof | 🟡 |
| 66 | Umbrellas, walking sticks, seat sticks, riding crops, whips, and parts thereof | 🟡 |
| 67 | Prepared feathers, down and articles thereof; artificial flowers; articles of human hair | 🟡 |
| 68 | Articles of stone, plaster, cement, asbestos, mica or similar materials | 🟢 |
| 69 | Ceramic products | 🟢 |
| 70 | Glass and glassware | 🟢 |
| 71 | Pearls, precious stones, metals, coins, etc. | 🟢 |
| 72 | Iron and steel | 🟢 |
| 73 | Articles of iron and steel | 🟢 |
| 74 | Copper and articles thereof | 🟢 |
| 75 | Nickel and articles thereof | 🟢 |
| 76 | Aluminum and articles thereof | 🟢 |
| 77 | Lead and articles thereof | 🟢 |
| 78 | Zinc and articles thereof | 🟢 |
| 79 | Tin and articles thereof | 🟢 |
| 80 | Other base metals; cermets; articles thereof | 🟢 |
| 81 | Tools, implements, cutlery, spoons and forks of base metal and parts thereof | 🟢 |
| 82 | Miscellaneous articles of base metal | 🟢 |
| 83 | Nuclear reactors, boilers, machinery and mechanical appliances; parts thereof | ⚫ |
| 84 | Electric machinery, equipment and parts; sound equipment; television equipment | ⚫ |
| 85 | Railway or tramway; locomotives, rolling stock, track fixtures and parts thereof; mechanical and electromechanical traffic signal equipment | ⚫ |

| | | |
|---|---|---|
| 86 | Vehicles (not railway, tramway, rolling stock); parts and accessories | ● |
| 87 | Aircraft, spacecraft, and parts thereof | ● |
| 88 | Ships, boats and floating structures | ● |
| 89 | Optical, photographic, cinematographic, measuring, checking, precision, medical or surgical instruments/apparatus; parts and accessories | ● |
| 90 | Clocks and watches and parts thereof | ● |
| 91 | Musical instruments; parts and accessories thereof | ● |
| 92 | Arms and ammunition, parts and accessories thereof | ● |
| 93 | Furniture; bedding, mattresses, cushions, etc.; other lamps and light fitting, illuminated signs and nameplates, prefabricate buildings | ● |
| 94 | Toys, games and sports equipment; parts and accessories | ● |
| 95 | Miscellaneous manufactured articles | ● |
| 96 | Works of art, collectors pieces and antiques | ● |

Table 1.1: **List of commodities of the WTM, according to the standard international classification HS1996, and associated codes, as provided by the BACI-Comtrade dataset.** In the first column we show the number representing each product. In the third column we divide such commodities in classes of similar traded items, each of them being represented by a different colored circle; colors are the same as reported in the dendrogram in Figure 1.6.

# Bibliography

[1] A.-L. Barabási, R. Albert (1999) 'Emergence of scaling in random networks', *Science* **286**, 509

[2] M. E. J. Newman (2003) 'The structure and function of complex networks', *SIAM Review* **45**, 167

[3] D. J. Watts, S. H. Strogatz (1998) 'Collective dynamics of "small-world" networks', *Nature* **393**, 440

[4] S. Fortunato (2010) 'Community detection in graphs', *Physics Reports* **486** (3), 75

[5] S. Wasserman, K. Faust (1994) 'Social network analysis', Cambridge University Press (Cambridge, New York)

[6] S. V. Buldyrev, R. Parshani, G. Paul, H. E. Stanley, S. Havlin (2010) 'Catastrophic cascade of failures in interdependent networks', *Nature* **464**, 1025

[7] F. Radicchi (2014) 'Driving interconnected networks to supercriticality' *Physical Review X* **4** (2), 021014

[8] M. Szell, R. Lambiotte, S. Thurner (2010) 'Multirelational organization of large-scale social networks in an online world', *Proceedings of the National Academy of Sciences USA* **107** (31), 13636

[9] A. Cardillo, J. Gómez-Gardeñes, M. Zanin, M. Romance, D. Papo, F. del Pozo, S. Boccaletti (2013) 'Emergence of network features from multiplexity', *Scientific Reports* **3**, 1344

[10] R. G. Morris, M. Barthelemy (2012) 'Transport on coupled spatial networks', *Physical Review Letters* **109** (12), 128703

[11] F. Battiston, V. Nicosia, V. Latora (2014) 'Structural measures for multiplex networks', *Physical Review E* **89** (3), 032804

[12] V. Nicosia, G. Bianconi, V. Latora, M. Barthelemy (2013) 'Growing multiplex networks', *Physical Review Letters* **111** (5), 058701

[13] J. Y. Kim, K.-I. Goh (2013) 'Coevolution and correlated multiplexity in multiplex networks', *Physical Review Letters* **111** (5), 058702

[14] V. Nicosia, G. Bianconi, V. Latora, M. Barthelemy (2014) 'Non-linear growth and condensation in multiplex networks' *Physical Review E* **90**(4), 042807

[15] A. Saumell-Mendiola, M. A. Serrano, M. Boguñá (2012) 'Epidemic spreading on interconnected networks', *Physical Review E* **86** (2), 026106

[16] S. Gomez, A. Diaz-Guilera, J. Gómez-Gardeñes, C. J. Perez-Vicente, Y. Moreno, A. Arenas (2013) 'Diffusion dynamics on multiplex networks', *Physical Review Letters* **110** (2), 028701

[17] J. Gómez-Gardeñes, I. Reinares, A. Arenas, L.-M. Floria (2012) 'Evolution of cooperation in multiplex networks', *Scientific Reports* **2**, 620

[18] E. Estrada, J. Gómez-Gardeñes (2014) 'Communicability reveals a transition to coordinated behavior in multiplex networks', *Physical Review E* **89** (4), 042819

[19] M. E. J. Newman, S. H. Strogatz, D. J. Watts (2001) 'Random graphs with arbitrary degree distributions and their applications', *Physical Review E* **64** (2), 026118

[20] J. Park, M. E. J. Newman (2003) 'Origin of degree correlations in the Internet and other networks', *Physical Review E* **68** (2), 026112

[21] G. Bianconi (2013) 'Statistical mechanics of multiplex networks: entropy and overlap', *Physical Review E* **87** (6), 062806

[22] M. Barigozzi, G. Fagiolo, D. Garlaschelli (2010) 'Multinetwork of international trade: a commodity-specific analysis', *Physical Review E* **81** (4), 046104

[23] V. Nicosia, V. Latora (2015) 'Measuring and modelling correlations in multiplex networks', *Physical Review E* **92** (3), 032805

[24] K.-M. Lee, J. Y. Kim, W.-K. Cho, K.-I. Goh, I.-M. Kim (2012) 'Correlated multiplexity and connectivity of multiplex random networks', *New Journal of Physics* **14**, 033027

[25] D. Garlaschelli (2009) 'The weighted random graph model', *New Journal of Physics* **11**, 073005

[26] A. Barrat, M. Barthelemy, A. Vespignani (2008) 'Dynamical processes on complex networks', Cambridge University Press (Cambridge)

[27] B. Min, S. Do Yi, K.-M. Lee, K.-I. Goh (2014) 'Network robustness of multiplex networks with interlayer degree correlations', *Physical Review E* **89** (4), 042811

[28] J. Park, M. E. J. Newman (2004) 'Statistical mechanics of networks', *Physical Review E* **70** (6), 066117

[29] D. Garlaschelli, M. I. Loffredo (2008) 'Maximum likelihood: extracting unbiased information from complex networks', *Physical Review E* **78** (1), 015101

[30] T. Squartini, D. Garlaschelli (2011) 'Analytical maximum-likelihood method to detect patterns in real networks', *New Journal of Physics* **13**, 083001

[31] T. Squartini, R. Mastrandrea, D. Garlaschelli (2015) 'Unbiased sampling of network ensembles', *New Journal of Physics* **17**, 023052

[32] S. Maslov, K. Sneppen (2002) 'Specificity and stability in topology of protein networks', *Science* **296**, 910

[33] M. A. Serrano, M. Boguñá (2005) 'Weighted configuration model', *AIP Conference Proceedings* **776**, 101

[34] T. Squartini, F. Picciolo, F. Ruzzenenti, D. Garlaschelli (2013) 'Reciprocity of weighted networks', *Scientific Reports* **3**, 2729

[35] D. Garlaschelli, M. I. Loffredo (2004) 'Patterns of link reciprocity in directed networks', *Physical Review Letters* **93** (26), 268701

[36] R. Mantegna (1999) 'Hierarchical structure in financial markets', *European Physics Journal B* **11** (1), 193